Resource Allocation and Trajectory Optimization for UAV-Enabled Multi-User Covert Communications

***Abstract*—In this correspondence, covert air-to-ground communication is investigated to hide the wireless transmission from unmanned aerial vehicle (UAV). The warden's total detection error probability with limited observations is first analyzed. Considering the location uncertainty of the warden, a robust resource allocation and UAV trajectory optimization problem with worst-case covertness constraint is then formulated to maximize the average covert rate. To solve this optimization problem, we propose a block coordinate descent method based iterative algorithm to optimize the time slot allocation, power allocation and trajectory alternately. Numerical results demonstrate the effectiveness of the proposed algorithm in covert communication for UAVs.**

***Index Terms*—Covert communication, resource allocation, trajectory optimization, unmanned aerial vehicle.**

I. Introduction

With the advantages of flexible deployment, high mobility and clear line-of-sight (LoS) air-to-ground channels, unmanned aerial vehicle (UAV) assisted wireless communications have been widely used in both civil and military applications, including disaster rescue, surveillance, data gathering, as well as data relaying [1]. Due to the broadcast nature of wireless communications and the LoS air-to-ground links, UAV-enabled communications are more vulnerable to malicious eavesdroppers or wardens [2]. Physical layer security (PLS) is a promising technique to guarantee the secrecy of data transmission in UAV-enabled systems, and is shown effective with carefully designed transmit power and trajectory [2]–[4].

Although PLS can prevent the information from being decoded by eavesdroppers, there also exists the requirement of hiding the UAV transmission in some critical applications. For instance, in military applications, even the existence of transmission may arouse suspicion. Then, the communication may be positioned and attacked. In order to guarantee security, the existence of confidential wireless transmission should not be noticed by the adversary. For this purpose, covert communication, also known as low probability of intercept communication, has been investigated recently [5], [6]. For the covertness of UAV-assisted communication systems, good LoS air-to-ground channels result in higher detection probability by the warden. For instance, the detection of UAV's transmission was investigated in [7], with the total detection error probability analyzed. With the UAV working as a warden, the transmit power and number of hops were optimized to improve the covertness of a multi-hop system [8]. The covertness of an air-to-ground wireless system was analyzed in [9], where the UAV's transmit power and height were jointly optimized. The UAV's transmit power and trajectory were jointly optimized to maximize the covert throughput of air-to-ground communications in [10], where the warden was assumed to have an infinite number of observations in each time slot. These works have shown that the covertness of air-to-ground communications can be significantly improved by properly allocating radio resource of UAVs and exploiting their flexible trajectory. However, existing studies mainly consider the scenario of covert transmission to a single user, and the problem of exploiting UAV's mobility to serve multiple users covertly still remains unsolved. As indicated in [11], by exploiting the mobility of UAV to fly close to each user, more gains can be achieved when communicating with multiple users. Furthermore, time-division multiple access can be adopted to serve multiple users, where the time slots are allocated to the target user when the UAV flies close to it. By the time slot allocation, trajectory design, as well as power allocation, the covert transmission rate can be enhanced significantly.

Motivated by this, we consider covert communication with one UAV transmitting data to multiple ground users, where a terrestrial warden attempts detect the transmission of UAV using a limited number of observations. The warden is able to obtain the perfect location of UAV, whereas the UAV only has the estimated location of the warden. To guarantee robust covert communication, the worst-case average covert rate is maximized by jointly optimizing the time slot, transmit power and trajectory. To solve this non-convex problem, the covertness constraint is analyzed from the warden's and the UAV's point of view, respectively. Then, a block coordinate

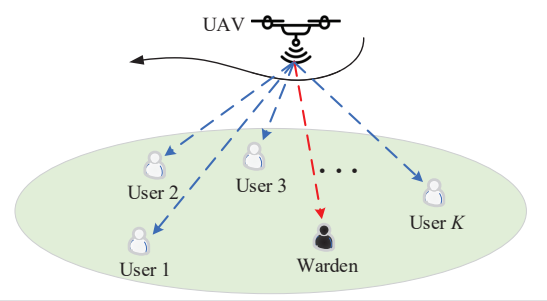

Fig. 1. UAV-enabled multi-user covert communication with a ground warden.

descent (BCD) method based iterative algorithm is proposed to solve the problem for low complexity.

II. System Model

Consider a communication system as shown in Fig. 1, where a flying UAV is transmitting confidential data to K ground users. At the same time, a warden on the ground is monitoring the transmission of UAV. Therefore, the UAV tries to hide its transmission from the warden. Without loss of generality, the Cartesian coordinate system is employed to describe the positions of these nodes. For the kth ground user, its horizontal coordinate can be expressed as $\mathbf{s}_k = (x_k, y_k)^T$. The horizontal location of the warden is $\mathbf{w} = (x_w, y_w)^T$. Assume that the UAV serves the K ground users within a time period of T. For ease of trajectory optimization, the flight period T is equally divided into N time slots, where N is large enough to guarantee that the position of UAV can be seen as approximately unchanged during each time slot. Although a large N is helpful to improve the accuracy, it is worth noting that larger value of N will result in higher computational complexity [11]. Thus, there exists a tradeoff between the accuracy and complexity.

At the nth time slot, the UAV's horizontal location can be expressed as $\mathbf{q}_u[n] = (x[n], y[n])^T$. Besides, the UAV's initial location $\mathbf{q}_I$ and final location $\mathbf{q}_F$ are fixed according to the UAV's task or takeoff/landing locations. As such, we have

$$\mathbf{q}_u[1] = \mathbf{q}_I, \quad \mathbf{q}_u[N] = \mathbf{q}_F. \tag{1}$$

Assuming that the UAV has constant speed in each time slot, and the maximum flying speed of UAV is V_{max}, we have

$$||\mathbf{q}_u[n+1] - \mathbf{q}_u[n]||^2 \leq (V_{max}T/N)^2, n = 1, \cdots, N-1. \tag{2}$$

We assume that the UAV flies at a fixed altitude H. In general, H is properly selected to avoid obstacles and provide LoS links with ground nodes. Although the probabilistic LoS model provides good approximation of the air-ground channel [12], [13], it is non-trivial to design the UAV trajectory with this model. As discussed in [14], we employ the LoS channel model for trajectory optimization, which has been widely adopted due to its tractability for trajectory design and good approximation when the UAV altitude is sufficiently high. Since the energy of the LoS component is much higher than that of the non-LoS (NLoS) component, the multipath fading can be neglected. Consider the single antenna scenario, the channel gains from the UAV to the kth user and from the UAV to the warden at time slot n can be expressed as

$$h_{uk}[n] = \frac{\beta}{||\mathbf{q}_u[n] - \mathbf{s}_k||^2 + H^2}, \ \forall k, \tag{3}$$

$$h_{uw}[n] = \frac{\beta}{||\mathbf{q}_u[n] - \mathbf{w}||^2 + H^2}, \tag{4}$$

where β is the reference channel gain at distance $d_0 = 1$ m. Note that the UAV's hovering fluctuation may influence the communication performance, especially when the UAV is equipped with a directional antenna [15]–[17]. In this correspondence, the UAV is assumed to have an isotropic antenna, and the effect of hovering fluctuation can be ignored for simplicity of analysis.

In covert communication, the warden detects whether the UAV is transmitting to the ground users. Since the UAV flies in the air, the warden is able to obtain its position at each time slot. Assume that the warden can only has limited number of observations during each time slot, i.e., the warden needs to decide whether the UAV is transmitting based on L times of sensing the received signal. During the nth time slot, the warden's lth received signal can be given by

$$y_w^{(l)}[n] = \begin{cases} n_w^{(l)}[n], & \mathcal{H}_0, \\ \sqrt{P[n]h_{uw}[n]}x^{(l)}[n] + n_w^{(l)}[n], & \mathcal{H}_1, \end{cases} \tag{5}$$

where $\mathcal{H}_0$ represents the null hypothesis that the UAV is not transmitting, while $\mathcal{H}_1$ represents the alternative hypothesis that the UAV is transmitting. $n_w^{(l)}[n]$ is the complex additive Gaussian noise at the warden. $P[n]$ is the transmit power of UAV at the nth time slot. $x^{(l)}[n]$ is the UAV's lth transmitted signal following complex Gaussian distribution with mean zero and variance 1. Therefore, the received signal at the warden follows

$$y_w^{(l)}[n] \sim \begin{cases} CN(0, \sigma^2), & \mathcal{H}_0, \\ CN(0, P[n]h_{uw}[n] + \sigma^2), & \mathcal{H}_1, \end{cases} \tag{6}$$

where σ^2 is the noise power.

By denoting $\mathcal{D}_0$ and $\mathcal{D}_1$ as the warden's decision in favor of $\mathcal{H}_0$ and $\mathcal{H}_1$, the false alarm probability of the warden can be expressed as $P_F[n] = \mathbb{P}(\mathcal{D}_1|\mathcal{H}_0)$, and the miss detection probability is $P_M[n] = \mathbb{P}(\mathcal{D}_0|\mathcal{H}_1)$. Consider that the warden assumes equal probability of $\mathcal{H}_0$ and $\mathcal{H}_1$, and then $\xi[n] = P_F[n] + P_M[n]$ is employed as the performance metric, as in [9] and [10]. The UAV's goal is to let the total error probability of warden $\xi[n]$ approximate to 1 in each time slot as

$$\xi[n] = P_F[n] + P_M[n] \geq 1 - \epsilon, \quad \forall n, \tag{7}$$

where $0 \leq \epsilon \leq 1$ is an sufficiently small positive value according to the covertness requirement.

The UAV serves the K ground users using time-division multiple access (TDMA), i.e., the UAV can only send message to at most one user in each time slot. We employ a binary variable $\alpha_k[n]$ to denote whether the kth user is served by the UAV in the nth time slot, i.e., the UAV is sending message to user k when $\alpha_k[n] = 1$, and otherwise $\alpha_k[n] = 0$. As such, the achievable rate of user k at the nth slot can be given by

$$R_k[n] = \alpha_k[n] \log_2 \left(1 + P[n]h_{uk}[n]/\sigma^2\right), \tag{8}$$

where $\alpha_k[n]$ satisfies $\sum_{k=1}^{K}\alpha_k[n]\leq 1$.

III. Problem Formulation

In this correspondence, our goal is to maximize the average covert rate of each user, i.e., $\frac{1}{N}\sum_{n=1}^{N}R_k[n]$ under the covertness constraint (7), by optimizing the UAV's time slot allocation, transmit power, as well as trajectory. Let $\boldsymbol{\alpha}=\{\alpha_k[n]\},\ \forall k,n$, $\mathbf{P}=\{P[n]\},\ \forall n$, and $\mathbf{Q}=\{\mathbf{q}_u[n]\},\ \forall n$, and the problem is formulated as

$$\max_{\eta,\boldsymbol{\alpha},\mathbf{P},\mathbf{Q}}\quad \eta \tag{9a}$$

$$s.t.\quad \frac{1}{N}\sum_{n=1}^{N}\alpha_k[n]\log_2\left(1+\frac{P[n]h_{uk}[n]}{\sigma^2}\right)\geq\eta,\ \forall k, \tag{9b}$$

$$P_F[n]+P_M[n]\geq 1-\epsilon,\quad \forall n, \tag{9c}$$

$$\alpha_k[n]\in\{0,1\},\quad \forall k,n, \tag{9d}$$

$$\sum\nolimits_{k=1}^{K}\alpha_k[n]\leq 1,\quad \forall n, \tag{9e}$$

$$||\mathbf{q}_u[n+1]-\mathbf{q}_u[n]||^2=\left(V_{max}T/N\right)^2,\quad n=1,\cdots,N-1, \tag{9f}$$

$$\mathbf{q}_u[1]=\mathbf{q}_I,\ \mathbf{q}_u[N]=\mathbf{q}_F, \tag{9g}$$

$$0\leq P[n]\leq P_{max},\quad \forall n, \tag{9h}$$

where η is a slack variable, and P_{max} is the maximum transmit power of the UAV.

It can be seen that the problem in (9) is difficult to solve due to the non-convex constraints (9b) and (9c), and the integer constraint (9d). Specifically, (9c) is intractable due to the non-convex and complicated expression of the total error probability $\xi[n]$. In the following, to make (9c) more tractable, we first analyze the detection performance of warden. The worst-case covertness constraint (9c) from the UAV's point of view is then analyzed.

A. Constraint (9c) from Warden's Point of View

Denoting the L received signals at the warden as $\mathbf{Y}[n]=\{y_w^{(l)}[n]\},\ \forall l$, the likelihood function under $\mathcal{H}_0$ can be expressed as

$$f(\mathbf{Y}[n]|\mathcal{H}_0)=\frac{1}{\left(\sqrt{2\pi}\sigma\right)^L}\prod_{l=1}^{L}\exp\left(-\frac{\left|y_w^{(l)}[n]\right|^2}{2\sigma^2}\right). \tag{10}$$

Likewise, the likelihood function under $\mathcal{H}_1$ can be given by

$$f(\mathbf{Y}[n]|\mathcal{H}_1)=\frac{1}{\left(\sqrt{2\pi}\hat{\sigma}\right)^L}\prod_{l=1}^{L}\exp\left(-\frac{\left|y_w^{(l)}[n]\right|^2}{2\hat{\sigma}^2}\right), \tag{11}$$

where $\hat{\sigma}^2=P[n]h_{uw}[n]+\sigma^2$.

Following (10) and (11), the log-likelihood ratio can be denoted as

$$\begin{aligned}\mathcal{L}[n]&=\log\left(\frac{f(\mathbf{Y}[n]|\mathcal{H}_1)}{f(\mathbf{Y}[n]|\mathcal{H}_0)}\right)\\&=\frac{L}{2}\log\left(\frac{\sigma^2}{\hat{\sigma}^2}\right)+\frac{1}{2}\left(\frac{1}{\sigma^2}-\frac{1}{\hat{\sigma}^2}\right)\sum_{l=1}^{L}\left|y_w^{(l)}[n]\right|^2.\end{aligned} \tag{12}$$

Consider that the warden assumes equal probability of $\mathcal{H}_0$ and $\mathcal{H}_1$, the optimal decision of the warden can be given by

$$\mathcal{L}[n]\underset{\mathcal{D}_0}{\overset{\mathcal{D}_1}{\gtrless}}0. \tag{13}$$

Following (12) and (13), the optimal decision rule can be rewritten as

$$\mathcal{T}_w[n]\ \triangleq\sum_{l=1}^{L}\left|y_w^{(l)}[n]\right|^2\underset{\mathcal{D}_0}{\overset{\mathcal{D}_1}{\gtrless}}\tau\triangleq\frac{L\log\left(\frac{\hat{\sigma}^2}{\sigma^2}\right)}{\frac{1}{\sigma^2}-\frac{1}{\hat{\sigma}^2}}. \tag{14}$$

It is worth noting that $\mathcal{T}_w[n]$ can be regarded as the total received power of the L observations at the nth time slot, which can be obtained by a radiometer. Note that when the warden has prior knowledge of the UAV's communication protocol, better detection performance can be achieved [18]. However, since it is difficult for the warden to obtain the prior information of the UAV's covert transmission, we assume that the warden employs the most commonly used energy detection as in [5]–[10].

Under $\mathcal{H}_0$, we can conclude that $\mathcal{T}_w[n]$ follows Gamma distribution from (6), i.e., $\mathcal{T}_w[n]\sim\Gamma(L,\frac{1}{\sigma^2})$. The false alarm probability can be obtained from its complementary cumulative distribution function as

$$P_F[n]=1-\frac{\gamma(L,\frac{\tau}{\sigma^2})}{(L-1)!}, \tag{15}$$

where $\gamma(s,x)=\int_{-\infty}^{x}t^{s-1}e^{-t}\mathrm{d}t$ is the lower incomplete Gamma function.

Likewise, under $\mathcal{H}_1$ we have $\mathcal{T}_w[n]\sim\Gamma(L,\frac{1}{\hat{\sigma}^2})$. The miss detection probability can be obtained by the cumulative distribution function (CDF) of $\mathcal{T}_w[n]$ as

$$P_M[n]=\frac{\gamma(L,\frac{\tau}{\hat{\sigma}^2})}{(L-1)!}. \tag{16}$$

In order to achieve covert communication, the constraint (9c) should be satisfied. However, we can see that $\xi[n]=P_F[n]+P_M[n]$ is highly complicated with respect to the variables $\mathbf{P}$ and $\mathbf{Q}$ in (9), which makes (9) non-trivial.

Fortunately, we find that $\xi[n]$ is non-increasing with respect to $\hat{\sigma}^2$. This can be proved by verifying that the derivative of $\xi[n]$ is non-positive with respect to $\hat{\sigma}^2$, the detail of which is omitted for brevity. The maximum value of $\hat{\sigma}^2$ satisfying (9c) can be represented as $\hat{\sigma}_m^2$, and it can be numerically obtained by bisection search. As such, (9c) can be transformed as

$$P[n]h_{uw}[n]\leq\hat{\sigma}_m^2-\sigma^2. \tag{17}$$

B. Constraint (9c) from UAV's Point of View

As clarified in [10], the location of the warden can be estimated by UAV-mounted cameras or radars. Since neutralizing the warden physically may arouse suspicion from the adversary, it is better to hide the existence of UAV's transmission. Different from [13] that achieves the PLS with unknown location information of the adversary, we consider the robust UAV covert communication under the worst-case of the warden's location estimation error. The location of the warden can be expressed at the UAV's point of view as

$$\mathbf{w}=\hat{\mathbf{w}}+\mathbf{e}_w, \tag{18}$$

where $\hat{\mathbf{w}} = (x_e, y_e)^T$ is the estimated position of the warden, and $\mathbf{e}_w = (\Delta x, \Delta y)^T$ is the estimation error.

Assume that the warden locates at a circular region centered at $\hat{\mathbf{w}}$ with radius r, and the estimation error $\mathbf{e}_w$ follows

$$||\mathbf{e}_w||^2 - r^2 \leq 0. \tag{19}$$

Considering the worst-case covert communication, (17) is equivalent to the following constraint for any possible location of the warden.

$$-||\mathbf{q}_u[n] - \hat{\mathbf{w}} - \mathbf{e}_w||^2 + \frac{P[n]\beta}{\hat{\sigma}_m^2 - \sigma^2} \leq 0. \tag{20}$$

The worst-case covertness constraint implies that (19) is a subset of the constraint (20) with respect to $\mathbf{e}_w$. Since there exists at least one point that (19) strictly holds, the following constraint is equivalent to the worst-case covertness constraint, according to the S-procedure.

$$\Phi[n] = \begin{bmatrix} \mu[n]+1 & 0 & x_e - x[n] \\ 0 & \mu[n]+1 & y_e - y[n] \\ x_e - x[n] & y_e - y[n] & z[n] - r^2\mu[n] \end{bmatrix} \succeq 0, \tag{21}$$

where $\mu[n] \geq 0$, $z[n] = ||\mathbf{q}_u[n] - \hat{\mathbf{w}}||^2 - \frac{P[n]\beta}{\hat{\sigma}_m^2 - \sigma^2}$.

IV. Covert Rate Maximization

Using results from the previous section, a BCD based iterative algorithm is proposed to solve the problem (9) approximately.

A. Time Slot Allocation

With fixed $\mathbf{P}$ and $\mathbf{Q}$, (9) can be rewritten as

$$\begin{aligned} \max_{\eta, \boldsymbol{\alpha}} \quad & \eta \\ s.t. \quad & \text{(9b), (9d), (9e).} \end{aligned} \tag{22}$$

With the integer constraint (9d), (22) is still intractable. We relax $\boldsymbol{\alpha}$ into continuous ones as

$$0 \leq \hat{\alpha}_k[n] \leq 1, \ \forall k, n. \tag{23}$$

By defining $\hat{\boldsymbol{\alpha}} = \{\hat{\alpha}_k[n]\}$, $\forall k, n$, (22) can be rewritten as

$$\begin{aligned} \max_{\eta, \hat{\boldsymbol{\alpha}}} \quad & \eta \\ s.t. \quad & \text{(9b), (9e), (23).} \end{aligned} \tag{24}$$

Problem (24) is a linear optimization, which can be solved using the interior-point method [19].

B. Power Allocation

Note that for the fixed trajectory $\mathbf{Q}$, the constraint (9c) in the worst case is given as

$$P[n] \leq \frac{(\hat{\sigma}_m^2 - \sigma^2)\left(D[n] + H^2\right)}{\beta}, \tag{25}$$

where

$$\begin{aligned} D[n] &= \min_{||\mathbf{e}_w||^2 - r^2 \leq 0} ||\mathbf{q}_u[n] - \hat{\mathbf{w}} - \mathbf{e}_w||^2 \\ &= \begin{cases} 0, & ||\mathbf{q}_u[n] - \hat{\mathbf{w}}||^2 \leq r^2, \\ (d[n] - r)^2, & ||\mathbf{q}_u[n] - \hat{\mathbf{w}}||^2 > r^2. \end{cases} \end{aligned} \tag{26}$$

In (26), $d[n] = \sqrt{||\mathbf{q}_u[n] - \hat{\mathbf{w}}||^2}$.

With fixed $\hat{\boldsymbol{\alpha}}$ and $\mathbf{Q}$, the transmit power optimization can be given by

$$\begin{aligned} \max_{\eta, \mathbf{P}} \quad & \eta \\ s.t. \quad & \text{(9b), (9h), (25).} \end{aligned} \tag{27}$$

Problem (27) is convex, which can be solved by the interior-point method.

C. Trajectory Optimization

With fixed $\hat{\boldsymbol{\alpha}}$ and $\mathbf{P}$, by defining $\boldsymbol{\mu} = \{\mu[n]\}$, $\forall n$, the trajectory optimization is given by

$$\begin{aligned} \max_{\eta, \mathbf{Q}, \boldsymbol{\mu}} \quad & \eta && \text{(28a)} \\ s.t. \quad & \Phi[n] \succeq 0, \quad \forall n, && \text{(28b)} \\ & \mu[n] \geq 0, \quad \forall n, && \text{(28c)} \\ & \text{(9b), (9f), (9g).} \end{aligned}$$

Since (9b) and (28b) are non-convex constraints, (28) is non-convex. Note that $R_k[n]$ on the left hand side of (9b) is convex with respect to $d_k[n] \triangleq ||\mathbf{q}_u[n] - \mathbf{s}_k||^2 + H^2$. Since the first-order Taylor series of a convex function is its global lower bound, given UAV location $\mathbf{q}_u^\nu[n]$, we have

$$\begin{aligned} R_k[n] &\geq A_{1k}[n] - A_{2k}[n]\left(||\mathbf{q}_u[n] - \mathbf{s}_k||^2 - ||\mathbf{q}_u^\nu[n] - \mathbf{s}_k||^2\right) \\ &\triangleq R_k^{LB}[n], \end{aligned} \tag{29}$$

where $A_{1k}[n] = \log_2\left(1 + P[n]\beta/\left(d_k[n]\sigma^2\right)\right)$ and $A_{2k}[n] = \frac{P[n]\beta/\sigma^2 \log_2 e}{d_k[n](d_k[n] + P[n]\beta/\sigma^2)}$.

In (28b), $z[n]$ is nonlinear with respect to $\mathbf{q}_u[n]$, but convex. With given UAV location $\mathbf{q}_u^\nu[n]$, we have

$$z[n] \geq b_1[n] + \mathbf{b}_2^T[n]\left(\mathbf{q}_u[n] - |\mathbf{q}_u^\nu[n]\right) \triangleq z^{LB}[n], \tag{30}$$

where $b_1[n] = ||\mathbf{q}_u^\nu[n] - \hat{\mathbf{w}}||^2 - \frac{P[n]\beta}{\hat{\sigma}_m^2 - \sigma^2}$ and $\mathbf{b}_2[n] = 2\left(\mathbf{q}_u^\nu[n] - \hat{\mathbf{w}}\right)$.

Based on (29) and (30), the problem (28) can be approximated as

$$\begin{aligned} \max_{\eta, \mathbf{Q}, \boldsymbol{\mu}} \quad & \eta && \text{(31a)} \\ s.t. \quad & \frac{1}{N}\sum_{n=1}^{N} R_k^{LB}[n] \geq \eta, \quad \forall k, n, && \text{(31b)} \\ & \hat{\Phi}[n] \succeq 0, \quad \forall n, && \text{(31c)} \\ & \text{(9f), (9g), (28c),} \end{aligned}$$

where

$$\hat{\Phi}[n] = \begin{bmatrix} \mu[n]+1 & 0 & x_e - x[n] \\ 0 & \mu[n]+1 & y_e - y[n] \\ x_e - x[n] & y_e - y[n] & z^{LB}[n] - r^2\mu[n] \end{bmatrix}. \tag{32}$$

Since $z^{LB}[n]$ is a lower bound of $z[n]$, we have $\Phi[n] \succeq \hat{\Phi}[n]$. Therefore, the solution to (31) is a feasible solution to (28). Note that (31) is a semi-definite programming problem, which can be efficiently solved by the interior-point method.

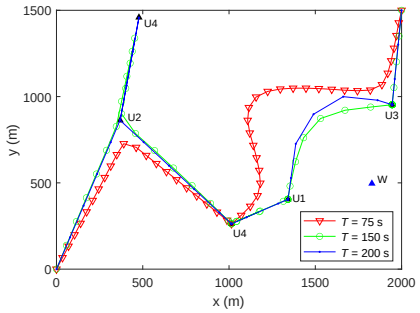

Fig. 2. Optimized trajectories for 5 users.

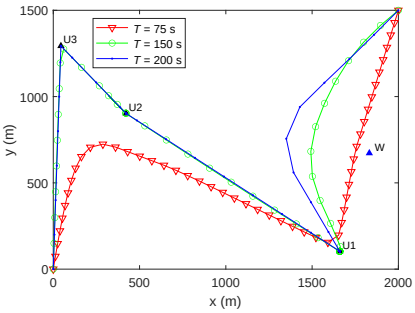

Fig. 3. Optimized trajectories for 3 users.

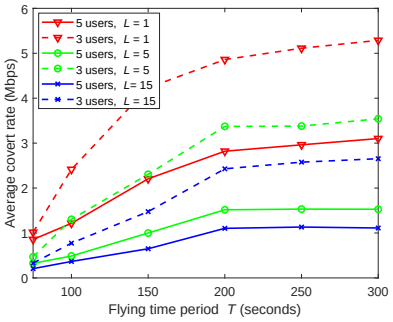

Fig. 4. Average covert rate versus T.

Algorithm 1 Iterative Algorithm for Solving Problem (9).

1: Let $\nu = 0$ and initialize the feasible $\mathbf{P}^\nu$, $\mathbf{Q}^\nu$, $0 < \theta^\nu \leq 1$ and the number of iterations I_m. We have $\theta_{step} = \frac{1-\theta^\nu}{I_m}$.
2: **repeat**
3: Solve the problem (24) with fixed $\mathbf{P}^\nu$ and $\mathbf{Q}^\nu$ to obtain the optimal solution as $\hat{\boldsymbol{\alpha}}^{\nu+1}$.
4: Solve the problem (27) with fixed $\hat{\boldsymbol{\alpha}}^{\nu+1}$ and $\mathbf{Q}^\nu$ to obtain the optimal solution as $\mathbf{P}^{\nu+1}$.
5: Update $\theta^\nu = \theta^\nu + \theta_{step}$.
6: Solve the problem (31) with fixed $\hat{\boldsymbol{\alpha}}^{\nu+1}$ and $\mathbf{P}^{\nu+1}$ to obtain the optimal solution as $\mathbf{Q}^{\nu+1}$.
7: Update $\nu = \nu + 1$.
8: **until** $\theta^\nu = 1$, and the fractional increase of the objective value is sufficiently small.
9: Reconstruct $\boldsymbol{\alpha}$ from $\hat{\boldsymbol{\alpha}}$ by (35).

D. Overall Algorithm

In the BCD method, one block of variables is optimized with the other blocks of variables fixed. However, when the optimal solution to (27) is achieved, the constraint (25) may hold with equality. In this case, the UAV may fail to update its trajectory by solving (31). To address this, a parameter θ assisted BCD algorithm is proposed. For $0 < \theta^\nu \leq 1$ in the νth iteration, the constraint (25) in the problem (27) is replaced by

$$P[n] \leq \frac{\theta^\nu(\hat{\sigma}_m^2 - \sigma^2)\left(D[n] + H^2\right)}{\beta}. \tag{33}$$

After solving (27), θ^ν is updated by $\theta^\nu = \theta^\nu + \theta_{step}$, where θ_{step} is properly selected to satisfy $\theta^\nu = 1$ at the end of iterations. As such, $b_1[n]$ in (30) can be replaced by

$$b_1[n] = ||\mathbf{q}_u^\nu[n] - \hat{\mathbf{w}}||^2 - \frac{P[n]\beta}{(\hat{\sigma}_m^2 - \sigma^2)\,\theta^\nu}. \tag{34}$$

After the iterations, the relaxed continuous variables $\hat{\boldsymbol{\alpha}}$ need to be converted into integer ones in the following way.

$$\alpha_k[n] = \begin{cases} 1 & \text{if} \quad k = \underset{i\in\{1,\cdots,K\}}{\arg\max}\ \hat{\alpha}_i[n], \\ 0 & \text{else.} \end{cases} \tag{35}$$

The overall algorithm is summarized in Algorithm 1. Since the objective function of (9) is non-decreasing and is upper-bounded by its optimal value, Algorithm 1 converges. Note that, in each iteration, three convex optimization problems are solved, and the order of complexity is $O(KN)^{3.5}$. It is also worth noting that Algorithm 1 is not guaranteed to converge to the global optimum. However, the numerical results in Section V will show the significant gain achieved by Algorithm 1.

V. Numerical Results

In this section, node distributions with 5 users and 3 users in an rectangular area of 2×1.5 km^2 are considered as shown in Fig. 2 and Fig. 3, respectively. The parameters are selected similar to [20], where the carrier frequency is 5 GHz, the bandwidth is 10 MHz, the noise power spectrum density is -169 dBm/Hz, $H = 100$ m, $V_{max} = 50$ m/s, $P_{max} = 0.1$ W, $N = 50$, $\mathbf{q}_I = (0, 0)^T$ and $\mathbf{q}_F = (2000, 1500)^T$. The initial trajectory is from $\mathbf{q}_I$ to $\mathbf{q}_F$ directly with uniform speed. The initial transmit power is the maximum power satisfies (25).

The optimized trajectories with 5 users and 3 users are shown in Fig. 2 and Fig. 3, where T is equal to 75 s, 100 s and 200 s, respectively. The parameters are chosen as $L = 5$, $\epsilon = 0.05$ and $r = 50$ m. We can see that as T increases, the UAV has more freedom to fly close to each user to achieve better air-ground channels. Usually, the UAV tends to fly away from the warden to avoid being detected. However in Fig. 2, when $T = 75$ s, the UAV is unable to hover above user 4 due to the limited T, and some of the slots when UAV is flying between user 1 and user 3 are allocated to user 4. Thus, the trajectory is far away from the warden and close to user 4 when $T = 75$ s. When $T = 200$ s, the UAV can fly above user 4 and allocate the enough slots to it. In addition, the UAV would like to spend less time with less transmit power to avoid being detected when it flies close to the warden. Accordingly, when more time is given, e.g., $T = 200$ s, the UAV can fly closer to the warden with much faster speed and less transmit power than the $T = 75$ s case. Therefore, in Fig. 2 when $T = 75$ s, the UAV flies closer to the warden than the $T = 200$ s case. The result in Fig. 2 is not a common case, and in Fig. 3 when $T = 75$ s, the UAV will always fly closer to the warden than the $T = 200$ s case.

In Fig. 4, the average covert rate versus T is demonstrated. The curves with $L = 1$, 5 and 15 are given. The parameters are chosen as $\epsilon = 0.05$ and $r = 50$ m. We can see that the average covert rate increases with T. This shows that when the UAV has more time to fly close to each target user, more gains of covert rate can be achieved. Besides, the 3-user case achieves

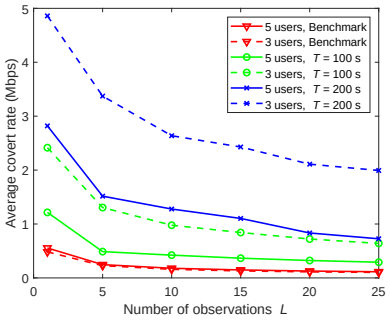

Fig. 5. Average covert rate versus L.

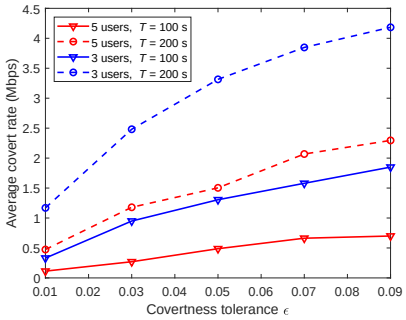

Fig. 6. Average covert rate versus ϵ.

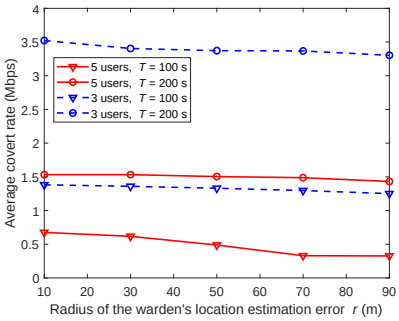

Fig. 7. Average covert rate versus r.

higher covert rate than the 5-user case. This is because more time are allocated to each user when there are fewer users. It is also observed that higher average covert rate can be achieved with smaller L.

Fig. 5 shows the average covert rate versus L. The curves with $T = 100$ s and 200 s are given. The parameters are chosen as $\epsilon = 0.05$ and $r = 50$ m. A benchmark with initial trajectory, initial transmit power, and optimized time slot allocation is given for comparison. We can see that the proposed algorithm has higher average covert rate for each value of L when compared with the benchmark. In addition, when L increases, the average covert rate decreases. This is because the warden can achieve better detection performance with more observations. It is also observed that the 3-user case achieves higher covert rate than the 5-user case.

The average covert rate versus the detection tolerance ϵ is shown in Fig. 6. The parameters are chosen as $r = 50$ m and $L = 5$. The results show that the covert rate increases with ϵ. The average covert rate versus the radius of warden's location estimation error r is shown in Fig. 7. The parameters are chosen as $\epsilon = 0.05$ and $L = 5$. The results show that the covert rate decreases slightly when r increases.

VI. Conclusion and Future Work

In this correspondence, the covert communication between a UAV and multiple ground users has been investigated. The total detection error probability with uncertain warden's location has been analyzed. Then, the worst-case covert communication problem has been formulated to maximize the average covert rate, by jointly optimizing the time slot allocation, transmit power and trajectory. To tackle this non-convex problem, a BCD based iterative algorithm has been proposed. Numerical results have shown that the proposed algorithm can efficiently improve the covert rate of the UAV-enabled network. In the future work, we will continue to focus on the scenario with multiple wardens and hovering fluctuation.

References

[1] Y. Zeng, R. Zhang, and T. J. Lim, "Wireless communications with unmanned aerial vehicles: opportunities and challenges," *IEEE Commun. Mag.*, vol. 54, no. 5, pp. 36–42, May 2016.

[2] M. Cui, G. Zhang, Q. Wu, and D. W. K. Ng, "Robust trajectory and transmit power design for secure UAV communications," *IEEE Trans. Veh. Technol.*, vol. 67, no. 9, pp. 9042–9046, Sep. 2018.

[3] F. Cheng, G. Gui, N. Zhao, Y. Chen, J. Tang, and H. Sari, "UAV-relaying-assisted secure transmission with caching," *IEEE Trans. Commun.*, vol. 67, no. 5, pp. 3140–3153, May 2019.

[4] W. Wang, J. Tang, N. Zhao, X. Liu, X. Y. Zhang, Y. Chen, and Y. Qian, "Joint precoding optimization for secure SWIPT in UAV-aided NOMA networks," *IEEE Trans. Commun.*, vol. 68, no. 8, pp. 5028–5040, Aug. 2020.

[5] B. A. Bash, D. Goeckel, D. Towsley, and S. Guha, "Hiding information in noise: fundamental limits of covert wireless communication," *IEEE Commun. Mag.*, vol. 53, no. 12, pp. 26–31, Dec. 2015.

[6] T. Zheng, H. Wang, D. W. K. Ng, and J. Yuan, "Multi-antenna covert communications in random wireless networks," *IEEE Trans. Wireless Commun.*, vol. 18, no. 3, pp. 1974–1987, Mar. 2019.

[7] J. Hu, Y. Wu, R. Chen, F. Shu, and J. Wang, "Optimal detection of UAV's transmission with beam sweeping in covert wireless networks," *IEEE Trans. Veh. Technol.*, vol. 69, no. 1, pp. 1080–1085, Jan. 2020.

[8] H. Wang, Y. Zhang, X. Zhang, and Z. Li, "Secrecy and covert communications against UAV surveillance via multi-hop networks," *IEEE Trans. Commun.*, vol. 68, no. 1, pp. 389–401, Jan. 2020.

[9] S. Yan, S. V. Hanly, I. B. Collings, and D. L. Goeckel, "Hiding unmanned aerial vehicles for wireless transmissions by covert communications," in *Proc. IEEE ICC*, Shanghai, China, May 2019, pp. 1–6.

[10] X. Zhou, S. Yan, J. Hu, J. Sun, J. Li, and F. Shu, "Joint optimization of a UAV's trajectory and transmit power for covert communications," *IEEE Trans. Signal Process.*, vol. 67, no. 16, pp. 4276–4290, Aug. 2019.

[11] Q. Wu, Y. Zeng, and R. Zhang, "Joint trajectory and communication design for multi-UAV enabled wireless networks," *IEEE Trans. Wireless Commun.*, vol. 17, no. 3, pp. 2109–2121, Mar. 2018.

[12] M. Alzenad, A. El-Keyi, and H. Yanikomeroglu, "3-D placement of an unmanned aerial vehicle base station for maximum coverage of users with different QoS requirements," *IEEE Wireless Commun. Lett.*, vol. 7, no. 1, pp. 38–41, Feb. 2018.

[13] H. Kang, J. Joung, J. Ahn, and J. Kang, "Secrecy-aware altitude optimization for quasi-static UAV base station without eavesdropper location information," *IEEE Commun. Lett.*, vol. 23, no. 5, pp. 851–854, May 2019.

[14] Y. Zeng, Q. Wu, and R. Zhang, "Accessing from the sky: A tutorial on UAV communications for 5G and beyond," *Proc. IEEE*, vol. 107, no. 12, pp. 2327–2375, Dec. 2019.

[15] M. T. Dabiri, H. Safi, S. Parsaeefard, and W. Saad, "Analytical channel models for millimeter wave UAV networks under hovering fluctuations," *IEEE Trans. Wireless Commun.*, vol. 19, no. 4, pp. 2868–2883, Apr. 2020.

[16] S. Suman, S. Kumar, and S. De, "Impact of hovering inaccuracy on UAV-aided RFET," *IEEE Commun. Lett.*, vol. 23, no. 12, pp. 2362–2366, Dec. 2019.

[17] S. Suman and S. De, "Optimal UAV-aided RFET system design in presence of hovering inaccuracy," *IEEE Trans Commun.*, vol. 69, no. 1, pp. 558–572, Jan. 2021.

[18] T. Yucek and H. Arslan, "A survey of spectrum sensing algorithms for cognitive radio applications," *IEEE Commun. Surveys Tuts.*, vol. 11, no. 1, pp. 116–130, 1st Quart. 2009.

[19] S. Boyd and L. Vandenberghe, *Convex Optimization*. Cambridge University Press, 2004.

[20] Y. Zeng, R. Zhang, and J. L. Teng, "Throughput maximization for UAV-enabled mobile relaying systems," *IEEE Trans. Commun.*, vol. 64, no. 12, pp. 4983–4996, Dec. 2016.